Organ/Tissue Doses Measured with Solid-State Integrating Dosemeters in a Low-Earth-Orbit Space Misson

H. Yasuda[1], T. Komiyama[2], G. D. Badhwar[3], and K. Fujitaka[1]
[1] National Institute of Radiological Sciences, Inage-ku, Chiba 263-8555, Japan
[2] National Space Development Agency of Japan, Tsukuba-shi, Ibaraki 305-8505, Japan
[3] NASA Lyndon B. Johnson Space Center, Houston, TX 77058-3696, U.S.A.

INTRODUCTION

For future space missions at the International Space Station, health risk to astronauts caused by space radiation needs to be properly quantified and controlled. The radiation field in space is low-dose rate, but the accumulated dose can be high during long-term missions *(1)*. Radiological risk under such a low dose-rate exposure, i.e. stochastic effect, has generally been evaluated using the quantity "effective dose equivalent" *(2)*. Whereas another quantity of "effective dose" has been introduced by ICRP in 1990 *(3)*, this concept is not used in the present study since it is technically difficult to determine the values of radiation weighting factor (w_R) for all particle species of isotropic space radiation. The effective dose equivalent can be obtained by summing up the absorbed doses in organs and tissues, weighted by both radiation quality and the relative sensitivity of each organ or tissue. Internal organ and tissue doses in a human body, however, have never been measured in past space missions; absorbed doses in only the brain were measured using a phantom head with thermoluminescent dosemeters (TLD) of LiF *(4)*. Thus, it is desired to directly measure organ and tissue doses using a life-size human phantom at the ISS orbit, not only for evaluation of the effective dose equivalent, but also for verification of the on-going model predictions using anatomical models *(5, 6)* and transport codes *(7, 8)*.

In order to measure the doses in internal organs and tissues in a phantom, we depend on small-scale passive detectors to avoid disturbing a radiation field by the reactions different from those in tissues. Such solid-state detectors have also advantages of long-term stability and simplicity in handling *(9)*. It is known, however, that the responses of TLDs show dependence on LET or particle energy *(10-12)*. In the present study, changes of the TL efficiencies to HZE particles are quantified at particle accelerators before using the TLDs in space.

MATERIALS AND METHODS

The detector system employed herein is a combination of TLD-Mg_2SiO_4:Tb (TDMS) (MSO-disk, Kasei Optonics Inc.) and plastic nuclear track detector (PNTD) (HARZLAS TD-1, Fukuvi Chemical Industry). The dimensions of the TDMS are $3.2\times3.2\times0.5$ mm^3 and those of the PNTD are $3.2\times16\times1.5$ mm^3. Although photoelectric interactions are expected for TDMS because of its high effective atomic number (11.1), these reactions are assumed to be negligible in space, since there are few low-energy photons relative to high-energy charged particles *(13)*. The combination of Mg_2SiO_4:Tb and PNTD had been proposed by Doke et al. *(14)* and used in past space missions *(14-16)*; however, they had not fully examined the TL efficiency of Mg_2SiO_4:Tb for heavy charged particles (HCP).

Ground calibration

Four chips each of TDMS and PNTD were packed in a rectangular case of tissue-equivalent resin (Toughwater phantom, Kyoto-kagaku Inc.) with dimensions of $80\times80\times6$ mm^2 including a cover of 2 mm thickness. Before radiation exposure for calibration, TDMS chips were annealed at 400 °C for 1 hour, followed by a fast quench to room temperature at a rate of about 50 °C min^{-1}. The detector cases were exposed to 10, 50, and 100 mGy·H_2O of selected HCP beams; these dose levels can be experienced by the astronauts who will stay in ISS for several months *(1, 13)*. The absorbed doses of all heavy ions and γ-rays were consistently measured using an air-filled ion chamber calibrated to standard radiation sources. The energies and the unrestricted LET values for water (LET_∞·H_2O; abbreviated to LET) of the HCP beams are summarized in Table 1. The detectors were exposed to the proton beam at the Cyclotron of National Institute of Radiological Sciences (NIRS-Cyclotron), to the Fe beam with energy of 1087 MeV amu^{-1} at the Alternating Gradient Synchrotron of Brookhaven National Laboratory (BNL-AGS), and to other particles (He, C, Ne, Si, Ar, and Fe) at the Heavy Ion Medical Accelerator in Chiba of NIRS (NIRS-HIMAC). The TDMS chips were also exposed to the same doses of ^{137}Cs γ-rays in NIRS within one day of each HCP irradiation. Selected heavy-ion beams were used to expose PNTD chips at angles from 0° to 90° in intervals of about 5 degrees.

Table 1. Conditions of heavy charged particle beams used for detector calibration. PNTD were exposed to 10 mGy of selected ions with asterisks (*); TDMS were exposed to 10, 50, and 100 mGy·H_2O of the beams without asterisks.

Particle	Beam energy at exit [MeV amu^{-1}]	Beam energy at target [a] [MeV amu^{-1}]	LET_∞·H_2O at target [b] [keV μm^{-1}]
H	70	65	1.0
He	150	140	2.2
He*	150	78	3.5**
He*	150	50	5.0**
C*	430	413	11
C*	290	271	14
C*	290	84	30**
Ne*	400	374	32
Ne*	230	193	45
Si*	490	460	55
Si*	490	230	80**
Si*	490	140	110**
Si*	490	102	140**
Ar	550	520	86
Fe	1087	1060	148
Fe	500	444	197
Fe*	500	120	420**

[a] The energies at the target position were estimated from the ranges measured with absorbers (Lucite) and an air-filled ion chamber.

[b] The LET_∞·H_2O of the particles with double asterisks (**) were used for only PNTD calibration; they were achieved by means of absorbers..

The TDMS chips were read 2 - 3 days after exposure with a heater-type reader (Kyokko TLD-Reader 2500, Kasei-Optonics Inc.). The integrated TL intensity of a main peak, from room temperature to 400 °C, was used for the absorbed-dose determination. The relative TL efficiency (ε) was calculated as the ratio of the TL intensities per unit absorbed dose between the samples exposed to HCP beam and those exposed to γ-rays. That is,

$$\varepsilon = \frac{TL_{HCP} / D_{HCP}}{TL_{\gamma} / D_{\gamma}} \quad , \qquad (1)$$

where TL_{HCP} and D_{HCP} are the TL intensity and the water absorbed dose, respectively, for a HCP beam; and TL_γ and D_γ are those for γ-rays. The PNTD chips were etched in 6N NaOH at 60 ºC for 12 hours. Etchpits on the PNTD surface were observed with an optical microscope and analyzed using an image-analysis program. The track-formation sensitivity (S) of PNTD was evaluated from the shape of an ellipse as follows *(17)*:

$$S = \frac{V_T}{V_B} - 1 = \sqrt{\frac{16 D_A^2 B^2}{(4B^2 - D_B^2)^2} + 1} - 1 \quad , \qquad (2)$$

where V_T is the etching rate along the track axis; V_B is the normal-surface (bulk) etching rate; D_A is the major axis of the etchpit ellipse; D_B is the minor axis; and B is the bulk-etching thickness. The B was measured with a micrometer as the difference in PNTD thickness between before and after etching. The incident angle (θ_i), defined as the angle between the beam direction and the detector plane, was estimated by *(17)*

$$\theta_i = \arcsin\left(\frac{4B^2 + D_B^2}{\sqrt{16D_A^2B^2 + (4B^2 - D_B^2)^2}}\right) \quad . \quad (3)$$

A particle with θ_i less than a certain angle (θ_c) cannot leave the track on the surface after etching. The θ_c is called the "critical incident angle", which is theoretically derived as follows *(18)*:

$$\theta_c = arcsin\left(\frac{V_B}{V_T}\right) = arcsin\left(\frac{1}{S+1}\right) \quad . \quad (4)$$

Spaceflight experiment

Three TDMS and two PNTD chips each from the same batch used in ground calibration were put into a case made of 1 mm-thick tissue-equivalent resin (Toughwater phantom, Kyotokagaku Inc.) with dimensions of 6.8×7.2×18 mm^3. Fifty-nine cases were inserted to selected organs and tissues in a life-size human phantom (RANDO Phantom, Alderson Research Laboratories) which is horizontally sliced at 3-cm intervals. The phantom is composed of tissue equivalent resin and a human skeleton *(19)*. The phantom was covered with a suite of heat-resistant fibers (Nomex, DuPont Inc.). Eight detector cases were put in the suit-pockets for measurements at breast and skin surface. The phantom was fixed with bungee cords onto a rack at the starboard side in the Spacehab Module of Space Shuttle "Discovery".

Discovery was launched from NASA Kennedy Space Center (KSC), Florida, at 18:10 June 2, as the 9th Shuttle-Mir Mission (STS-91). The Shuttle docked to the Russian Space Station Mir two days later (13:02, June 4) and, after orbiting the earth for about 4 days, undocked from Mir at 12:05, June 8. The mission continued for an additional 4 days until landing at KSC at 14:03 June 12. Total flight duration was 9.8 days. Background dose was measured with four non-launched control cases kept at NASA Johnson Space Center (JSC), Texas, during the flight. Thus, the doses additionally received in the space mission were evaluated in this experiment, whereas the background dose was estimated to be less than 2% of the total absorbed doses for all the cases. The phantom was returned immediately to JSC and the detector cases were removed there. All detector cases were sent to Japan and analyzed in NIRS, following the process described above for the ground calibration. The TL intensity (TL_{flight}) was converted to the ^{137}Cs-γ equivalent absorbed dose ($D_{\gamma\text{-}eq}$) as follows:

$$D_{\gamma-eq} = \frac{TL_{flight}}{TL_\gamma / D_\gamma} \quad . \quad (5)$$

The value of TL_γ/D_γ was given as an average of eight TDMS chips exposed to ^{137}Cs γ-rays; four samples to 2 mGy·H_2O and the others to 5 mGy·H_2O. The LET values for high-LET particles were evaluated with PNTD based on the relationship between S and LET. Whereas S is not directly related to LET but to the restricted energy loss (REL) for polymers *(14, 17, 20, 21)*, a ratio of REL to LET can be constant for the HCP with energy greater than several MeV amu^{-1}, i.e. dominant components of cosmic radiation *(22, 23)*.

RESULTS AND DISCUSSION

Ground calibration

Shown in Fig.1 is the relative TL efficiency (ε) of TDMS as a function of LET. The ε did not significantly change at less than 10 keV μm^{-1} from unity. At higher LET, however, the ε sharply decreased with increasing LET. The authors *(24)* have found a similar curve of the LET dependence for a different-shape Mg_2SiO_4:Tb. Such a reduction of ε would be attributed to saturation of luminescent centers. This phenomenon has successfully been explained *a priori* for other TLDs by means of target-hit models on the basis of track structure theory *(25-30)*. The shape of glow curve of TDMS did not change for these ions (the results are not shown here).

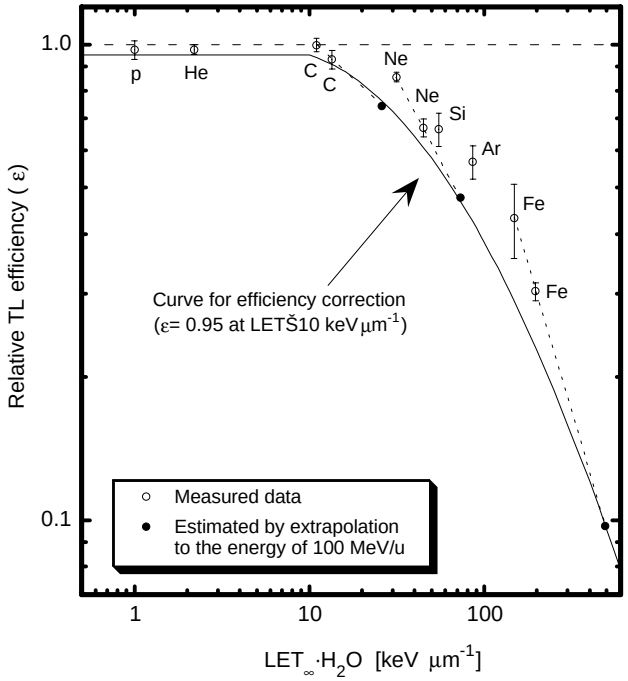

Fig. 1 Plots of relative TL efficiency of TLD-Mg_2SiO_4:Tb (TDMS) as ^{137}Cs-γ equivalent versus the unrestricted LET in water.

We can expect that reduction of ε for high-LET particles will be corrected according to the LET spectra evaluated with PNTD. The pattern of the ε-reduction, however, showed dependence on particle species as seen in Fig.1. This fact has been pointed out also for LiF in recent studies *(29, 30)*; they showed that the ε of LiF reduced to less than unity for HCP with LET > 10 keV μm^{-1}. For the purpose of radiological protection, ε values smaller than the actual values should be given not to underestimate absorbed doses and dose equivalents. Accordingly, we have employed an ε value less than unity (0.95) for the particles with LET ≥ 10 keV μm^{-1} (Fig.1). For the range of LET > 10 keV μm^{-1}, we assumed that predominant components are HZE particles in galactic cosmic rays (GCR) with energy greater than 100 MeV amu^{-1} *(23)*. Thus, the plots obtained for C, Ne, and Fe beams were linearly extrapolated to lower energy range in logarithmic scales and a regression curve was given for the plots estimated for 100 MeV amu^{-1} (See Fig.1).

Figure 2a shows the incident-angle dependence of track-formation sensitivity (S) of PNTD. No etchpit was observed for the particles having incident angles less than the values of critical angle (θ_c) derived from eqn (4). The S values, however, clearly decreased with lowering incident angle. This tendency appeared more strongly for the particles with lower LET, as observed in previous studies *(31, 32)*. Thus, we have given an empirical formula for correcting the error caused by incident-angle dependence of S as follows:

$$S = S_{90} - \frac{(90 - \theta_i)^a}{b \times S_{90}} \quad , \qquad (6)$$

where S_{90} is the S for a vertical incident beam; a and b are the constants. The regression curves of eqn (6) are shown in Fig.2a. The coefficients (a = 3.2 and b = 7.5×10^5) were determined through a fitting analysis. By solving eqn (6), we obtain the following formula to estimate the S_{90} from θ_i and S:

$$S_{90} = 0.5\times\left\{S+\sqrt{S^2+\frac{4\times(90-\theta_i)^a}{b}}\right\} \quad . \qquad (7)$$

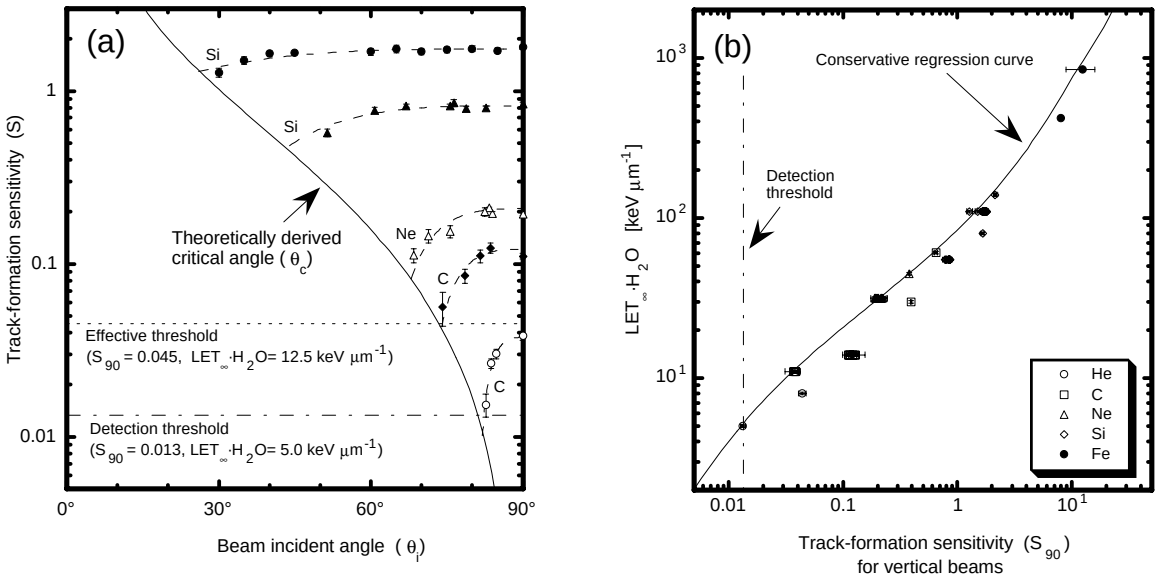

Fig. 2 The track-formation sensitivity, S, of PNTD as a function of the beam incident angle **(a)** and the unrestricted LET in water as a function of S for vertically incident beams **(b)**.

Figure 2b shows the plots of the LET versus the S_{90} values; these include the data in Fig.2a. We can see some fluctuations attributing to the conditions of the microscopy or the image-analysis program and, to some extent, skills of observers. It is reasonable that the S of a low-energy light ion is larger than that of a relativistic heavy ion at a similar level of LET, since S is not related directly to LET, but to the ionization density in the core of a track. Thus, in order to avoid underestimation of LET in keeping with radiological-protection practices, we have conservatively chosen a regression curve (a cubic function in the logarithmic scale) as indicated in Fig.2b.

Since no helium ions with LET equal to 3.5 keV μm^{-1} were detected, a detection threshold of 5.0 keV μm^{-1} (S= 0.013) was adopted in this study. Based on this value and the patterns of incident-angle dependence of S (Fig.2a), an effective threshold for isotropic space radiation was determined to be 12.5 keV μm^{-1} (S= 0.045). For the particles with lower LET, angular-dependent efficiency cannot be given on a theoretical basis.

Spaceflight experiment

When analyzing data from the PNTD flown in space, S and θ_i were estimated using eqns (2) and (3), respectively; the S was corrected to S_{90} using eqn (7); θ_c was calculated by eqn (4) for the S_{90} value. Figure 3a shows the cumulative planar-track fluence for position 1 in the 9.8-day Shuttle-Mir Mission. The measured data are plotted for the particles with LET > 12.5 keV μm^{-1}, i.e., the effective threshold LET, and the fluence in the range of 10 - 12.5 keV μm^{-1} has been estimated by a linear extrapolation from the data of 12.5 - 15 keV μm^{-1}. The plots of cumulative absorbed dose, dose equivalent, and estimated $D_{\gamma\text{-eq}}$ at position 1 (brain) are shown in Fig. 3b as a function of LET. The procedures for calculation of these quantities are stated in detail by Doke et al. *(14)*; we used the new Q-LET relationship recommended by ICRP in 1990 *(3)*. Since all the curves reach plateau around 100 keV μm^{-1}, we assumed that both a total absorbed dose and a total dose equivalent are accurately obtained without extrapolating the curves to a higher LET range. The $D_{\gamma\text{-eq}}$ values were 8-10 % lower than the total absorbed doses for almost all organs and tissues. In other words, TDMS has an efficiency greater than 90% in a spacecraft at the ISS orbit. Whereas Doke et al. *(14)* assumed that the efficiency of a different-shape Mg_2SiO_4:Tb is 0.6 for entire particles with LET > 3.5 keV μm^{-1}, the value (0.6) seems to be smaller than the actual one.

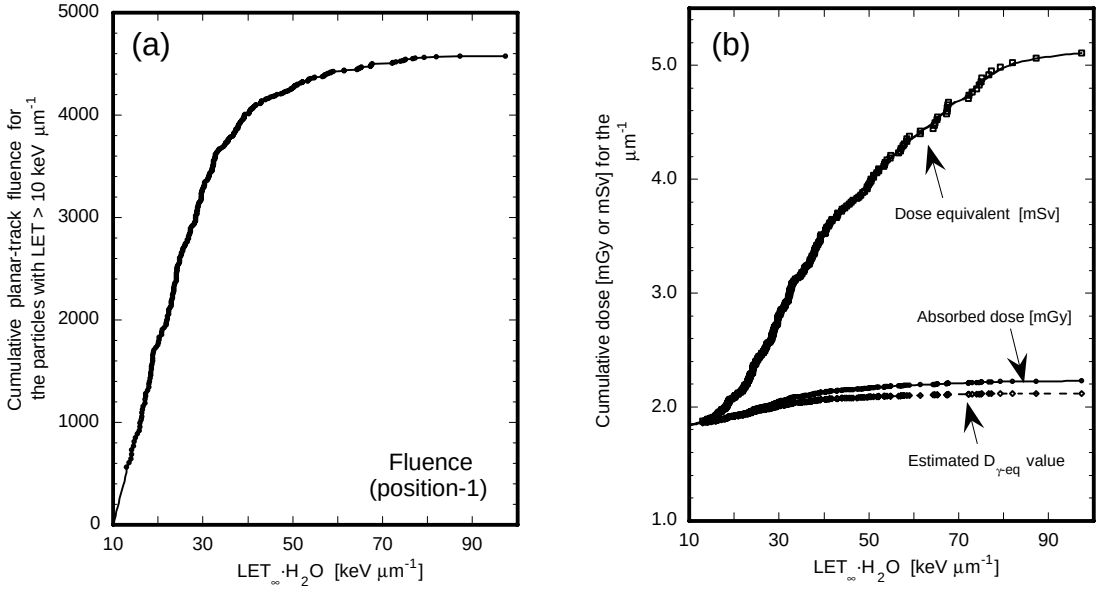

Fig. 3 The cumulative planar fluence measured with PNTD **(a)** and the cumulative plots of absorbed dose, dose equivalent, and ^{137}Cs-γ equivalent TDMS dose, $D_{\gamma\text{-eq}}$ **(b)** in the position 1 (brain) as a function of the unrestricted LET in water.

Summarized in Table 2 are the values of total absorbed dose, total dose equivalent, and effective quality factor (Q_e) calculated for each organ and tissue; the effective dose equivalent is also shown on the bottom line. The absorbed dose in or on the phantom during this 9.8-day low-earth-orbit mission ranged from 1.7 mGy to 2.7 mGy (factor = 1.6). The highest absorbed-dose values were observed at the shoulder-bone surface, stomach, liver, breast (chest); the lowest values at the colon, bone marrow, and bladder. The range in the dose equivalent was from 3.4 mSv (bone marrow and esophagus) to 5.2 mSv (shoulder-bone surface) by a factor of 1.5; and the effective quality factor (Q_e) ranged from 1.7 to 2.4 (factor= 1.4). Summing up these organ and tissue doses weighted by tissue weighting factors *(3)* (Table 2), we obtained the effective dose equivalent of 4.1 mSv; this value is about 90 % of the skin dose equivalent (H_{skin}). About half of the effective dose equivalent came from four internal organs: lung, stomach, bone marrow and colon, and other 23% from the gonad alone. As results, about 75% of the effective dose equivalent attributed to the five organs. The dose rate averaged over the entire flight duration (9.8 days) was about 0.4 mSv d^{-1}. This dose rate is smaller than the previously obtained values (0.6 – 0.8 mSv d^{-1}) in free-air conditions at almost the same orbit *(14-16, 33)*. A similar dose rate (about 0.4 mSv d^{-1}) was observed in a measurement using TEPC at the center of a polyethylene sphere with thickness of 12.7 g cm^{-2} *(34)*. These facts suggest that the phantom is efficiently a thick-shielding material.

Table 2. The values of absorbed dose, dose equivalent, and effective quality factor for organs and tissues, and the effective dose equivalent (the bottom line) in the 9.8-day Shuttle-Mir Mission (400 km×51.6°); the tissue weighting factors (w_T) and the w_T-weighted dose equivalents are also shown.

Organ or Tissue [c]	Absorbed dose (D_T) [mGy·H_2O] [b]	Organ or tissue dose equivalent (H_T) [mSv] [b]	Effective quality factor (Q_e) [b,c]	Tissue weighting factor (w_T)[c]	$H_T \times w_T$ [b]
Skin	2.2±0.17	4.5±0.05	2.0±0.16	0.01	0.05±0.001
Thyroid	2.2±0.12	4.0±0.21	1.9±0.16	0.05	0.20±0.011
Bone surface	2.7±0.24	5.2±0.22	1.9±0.12	0.01	0.05±0.002
Esophagus	2.1±0.13	3.4±0.49	1.7±0.17	0.05	0.17±0.024
Lung	2.1±0.31	4.4±0.76	2.1±0.20	0.12	0.53±0.091
Stomach	2.4±0.30	4.3±0.94	1.8±0.50	0.12	0.52±0.113
Liver	2.3±0.33	4.0±0.51	1.7±0.33	0.05	0.20±0.026
Bone marrow	1.8±0.10	3.4±0.40	1.9±0.14	0.12	0.41±0.048
Colon	1.7±0.22	3.6±0.42	2.2±0.44	0.12	0.43±0.050
Bladder	1.8±0.16	3.6±0.24	2.0±0.25	0.05	0.18±0.012
Gonad (Testis)	2.0±0.05	4.7±0.71	2.4±0.37	0.20	0.94±0.142
Breast (Chest)	2.3±0.16	4.5±0.11	1.9±0.13	0.05	0.23±0.006
Remainder	2.1±0.15	4.0±0.57	1.9±0.22	0.05	0.20±0.029
			Effective dose equivalent [mSv]:		4.1±0.22

[a] "Remainder" comprises brain, heart, spinal column, and rectum. Bone surface is at the shoulder. The dose at breast was measured in a Nomex-suit pocket on the chest; the skin dose was measured in another pocket on the abdomen.

[b] A value shows a mean (m) ± one standard deviation (σ); the σ indicates only the statistical error (type-A uncertainty).

[c] The Q-LET relationship and the w_T values were adopted from the 1990 recommendations of ICRP *(3)*.

We believe that the values in Table 2 appropriately include systematic errors (type-B uncertainty) in view of radiological protection, because the detector calibration curves (Figs. 1 and 2) are conservatively given. Assuming that degree of the type-B uncertainty is the same for all the data, we can see that the dose equivalents are significantly different among selected organs and tissues. The H_{skin} was higher than the dose equivalents (H_T) at many organs and tissues; large H_T values significantly higher than H_{skin} were observed only at the shoulder-bone surface and the brain. From these findings, one would expect that H_{skin} would conservatively indicate the individual dose of an astronaut; some overestimation is favorable for radiological-protection concerns. However, as the results of *t*-test, the H_T values in the lung, stomach, gonad, and breast – all of them are radiation sensitive - were not significantly different from the H_{skin} value. Accordingly, we note that such radiologically-important organs could have H_T values higher than H_{skin}, even though these organs are located deep inside a body. This fact suggests the possibility that an effective dose equivalent could be higher than H_{skin}. Whereas previous model calculations predict that the dose equivalent at a deep organ are always lower than that at skin surface *(35, 36)*, and they must be true for a simplified structure as polyethylene spheres *(34)*, the human body is surely different from such a small simple shape.

CONCLUSION

The first attempt to evaluate an effective dose equivalent in space was successfully done using a life-size human phantom in the 9th Shuttle-Mir Mission. The absorbed doses and the dose equivalents in organs and tissues varied by about 60 % over a human body. The skin dose equivalent (H_{skin}) on the abdomen was higher than the effective dose equivalent by about 10 %. It is thus expected that the individual dose of an astronaut can properly be measured at skin surface since a conservative evaluation is essential for the purpose of radiological protection. It should be noted, however, that the H_T values in deep organs or tissues are not necessarily higher than

H_{skin}; the H_T values at radiation-sensitive organs such as lung, stomach, gonad, and breast were not significantly different from the H_{skin}. We need to thoroughly measure internal dose distributions, particularly in such radiation-sensitive organs, before making a conclusion about the conservative feature of H_{skin}.

Since ISS will flow at almost the same orbit (400 km×51.6°) as Mir, the results in the present study are somewhat relevant to radiation doses received in future ISS missions. The values shown in Table 2, however, can vary by solar-activity change, shielding condition of a spacecraft, and the size and direction of a human body; they should affect the value of effective dose equivalent by changing the balance of particle species and energies. To quantify the effects of these modifying factors, we hope to repeat experiments using the life-size phantom in future ISS missions.

ACKNOWLEDGEMENTS

Sincere appreciation is expressed to Mr. Frank L. Gibbons, Lockeed Martin Corp., and Mr. Takahiro Abe, NASDA, for technical cooperation in the phantom experiment. The authors thank Ms. Sayaka Sato, Ms. Ayuchi Nakamura, Mr. Atsushi Kyan, Mr. Masashi Takada, and Dr. Yoshiya Furusawa, NIRS, for helpful assistance, and Dr. Mark R. Shavers, Baylor College of Medicine, for editorial comments. The Fe-beam irradiations at BNL-AGS were helped by Dr. Jack Miller, Lawrence Berkeley National Laboratory. Other heavy-ion irradiations were carried out as part of NIRS-HIMAC Research Project. The spaceflight experiment in S/MM-9 (STS-91) was greatly supported by NASDA and NASA.

REFERENCES

1. W. K. Sinclair, *History of development of radiation protection standards for space activities*. In NCRP Symposium Proc. 3 - Acceptability of Risk From Radiation -Application to Human Space Flight, pp.51-65, NCRP, Bethesda, MD, USA (1997).
2. International Commission on Radiological Protection (ICRP), *Recommendations of the International Commission on Radiological Protection*. Publ.26, Pergamon Press, Oxford, UK (1977).
3. International Commission on Radiological Protection (ICRP), *1990 Recommendations of the International Commission on Radiological Protection*. Publ.60, Pergamon Press, Oxford, UK (1990).
4. Konradi, W. Atwell, G. D. Badhwar, B. L. Cash, and K. A. Hardy, *Low earth orbit radiation dose distribution in a phantom head*. Nucl. Tracks Radiat. Meas. **20**, 49-54 (1992).
5. M. P. Billings and W. R. Yucker, *Summary of Final Report: The Computerized Anatomical Man (CAM) Model*. Report MDC-G4655, McDonnell Douglas Astronautics Company, Huntington Beach, CA, USA (1973).
6. W. R. Yucker and S. L. Huston, *Computerized Anatomical Female: Final Report*. Report MDC-H6107, McDonnell Douglas Astronautics Company, Huntington Beach, CA, USA (1990).
7. J. W. Wilson, L. W. Townsend, J. E. Nealy, S. Y. Chun, B. S. Hong, W. W. Buck, S. L. Lamkin, B. D. Ganapol, F. Khan, and F. A. Cucinotta, *BRYNTRN, A Baryon Transport Model*. NASA TP-2887, NASA, Washington, DC (1989).
8. J. W. Wilson, S. Y. Chun, F. F. Badavi, L. W. Townsend, and S. L. Lamkin, *HZETRN: A Heavy Ion/ Nucleon Transport Code for Space Radiations*. NASA TP-3146, NASA, Washington, DC (1991).
9. F. H. Attix, *Introduction to Radiological Physics and Radiation Dosimetry*. pp.395-411, John Wiley & Sons, New York (1986).
10. E. Tochilin, N. Goldstein, and J. T. Lyman, *The quality and LET dependence of three thermoluminescent dosemeters and their potential use as secondary standards*. In Proc. 2nd Int. Conf. on Luminescence, Washington, DC., pp.424-437 (1968).
11. W. Hoffman, and B. Prediger, *Heavy particle dosimetry with high temperature peaks of CaF_2:Tm and ^{7}LiF phosphors*. Radiat. Prot. Dosim. **6**, 149-152 (1984).
12. N. Vana, W. Schoner, M. Fugger, and Y. Akatov, *Absorbed dose measurement and LET determination with TLDs in space*. Radiat. Prot. Dosim. **66**, 145-152 (1996).
13. D. E. Robbins, *The space radiation environment*. In NCRP Symposium Proc. 3 - Acceptability of Risk From Radiation -Application to Human Space Flight, pp.5-32, NCRP, Bethesda, MD, USA (1997).
14. T. Doke, T. Hayashi, S. Nagaoka, K. Ogura, and R. Takeuchi, *Estimation of dose equivalent in STS-47 by combination of TLDs and CR-39*. Radiat. Meas. **24**, 75-82 (1995).
15. T. Hayashi, T. Doke, J. Kikuchi, J. Hasebe, G. D. Badhwar, S. Nagaoka, and M. Kato, *Measurement of LET distribution and dose equivalent on board the Space Shuttle STS-65*. Radiat. Meas. **26**, 935-945 (1996).

16. T. Hayashi, T. Doke, J. Kikuchi, T. Sakaguchi, R. Takeuchi, T. Takashima, M. Kobayashi, K. Terasawa, K. Takahashi, A. Watanabe, A. Kyan, N. Hasebe, T. Kashiwagi, K. Ogura, S. Nagaoka, M. Kato, T. Nakano, S. Takahashi, H. Yamanaka, K. Yamaguchi, and G. D. Badhwar, *Measurements of LET distribution and dose equivalent onboard the Space Shuttle IML-2 (STS-65) and S/MM#4 (STS-79)*. Biol. Sci. Space. **11**, 355-364 (1997).
17. K. Ogura, T. Doke, T. Kasuya, K. Kuwahara, M. Matsushima, S. Nagaoka, H. Ohnishi, T. Takahashi, H. Yamada, and F. Yatagai, *Determination of high LET cosmic particles' trajectories for space radiobiological studies*. Nucl. Tracks Radiat. Meas. **22**, 733-738 (1993).
18. G. F. Knoll, *Radiation Detection and Measurement*. pp.755-765, John Wiley and Sons. New York (1979).
19. International Commission on Radiation Units and Measurements (ICRU), *Tissue substitutes in radiation dosimetry and measurement*. ICRU Report 44, pp.20-38, ICRU, Bethesda, MD, USA (1989).
20. R. P. Henke, and E. V. Benton, *Charged particle tracks in polymers: No.3 - Range and energy loss tables*. USNRDL-TR-1102, U.S. Naval Radiological Defense Laboratory, San Francisco (1966).
21. E. V. Benton, *Charged particle tracks in polymers: No.4 – Criterion for track registration*. USNRDL-TR-67-80, U. S. Naval Radiological Defense Laboratory, San Francisco (1967).
22. J. A. Simpson, *Elemental and isotopic composition of the galactic cosmic rays*. Ann. Rev. Nucl. Part. Sci. **33**, 323-381 (1983).
23. National Council on Radiation Protection and Measurements (NCRP), *Guidance on Radiation Received in Space Activities*. NCRP Report 98, pp.15-26, NCRP, Bethesda, MD, USA (1989).
24. H. Yasuda and K. Fujitaka, *Responses of TLD-Mg_2SiO_4:Tb and Radiophoto-luminescent glass to heavy charged particles and space radiation*. Radiat. Prot. Dosim. **87**, 115-120 (2000).
25. L. Larsson and R. Katz, *Supralinearity of thermoluminescent dosimeters*. Nucl. Instrum. Meth. **138**, 631-636 (1976).
26. J. Kalef-Ezra and Y. S. Horowitz, *Heavy charged particle thermoluminescence dosimetry: track structure theory and experiments*. Int. J. Appl. Radiat. Isot. **33**, 1085-1100 (1982).
27. M. Moscovitch and Y. S. Horowitz, *A microdosimetric track interaction model applied to alpha particle induced supralinearity and linearity in thermoluminescent LiF:Mg,Ti*. J. Phys. D: Appl. Phys. **21**, 804-814 (1988).
28. L. Daling and R. Katz, *Thindown in lithium fluoride (TL-100*). Nucl. Sci. Tech. **2**, 147-152 (1991).
29. B. Geiss, M. Kramer, and G. Kraft, *Efficiency of thermoluminescent detectors to heavy charged particles*. Nucl. Instrum. Meth. **B142**, 592-598 (1998).
30. Avila, I. Gamboa-deBuen, and M. E. Brandan, *Study of the energy deposition in LiF by heavy charged particle irradiation and its relation to the thermoluminescent efficiency of the material*. J. Phys. D: Appl. Phys. **32**, 1175-1181 (1999).
31. T. Doke, T. Hayashi, M. Kobayashi, and A. Watanabe, *Dip angle dependence on track formation sensitivity in antioxidant doped CR-39 plates*. Radiat. Meas., **28**, 445-450 (1997).
32. H. Yasuda, Incident-angle dependency found in track formation sensitivity of a plastic nuclear track detector (TD-1). J. Health Phys.(Japan) **34**, 387-390 (1999).
33. G. D. Badhwar, M. J. Golightly, A. Konradi, W. Atwell, J. W. Kern, B. L. Cash, E. V. Benton, A. L. Frank, V. M. Petrov, I. V. Tchernykh, Yu A. Akatov, V. A. Shurshakov, V. V. Arkhangelsky, V. V. Kushin, N. A. Klyanchin, N. Vana, and W. Schoner, *In-flight radiation measurements on STS-60*. Radiat. Mes. **26**, 17-34 (1996).
34. G. D. Badhwar, P. M. O'Neill, and F. A. Cucinotta, *Depth-dose equivalent relationship for cosmic rays at various solar minima*. Radiat. Res. **134**, 9-15 (1993).
35. V. E. Dudkin and Yu V. Potapov, *Doses from galactic cosmic ray particles under spacecraft shielding*. Nucl. Tracks. Radiat. Meas. **20**, 33-39 (1992).
36. L. W. Townsend, F. A. Cucinotta, and J. W. Wilson, *Interplanetary crew exposure estimates for galactic cosmic rays*. Radiat. Res. **129**, 48-52 (1992).